Motion Control Systems with $\mathcal{H}^\infty$ Positive Joint Torque Feedback

Farhad Aghili, Martin Buehler, *Member, IEEE*, and John M. Hollerbach, *Fellow, IEEE*

***Abstract*—Positive joint torque feedback (JTF) can compensate the detrimental effects of load torques on position tracking performance. However, with (real world) nonideal torque sources, simple unity gain positive torque feedback can actually deteriorate the performance, or even result in instability. In this work, a new $\mathcal{H}^\infty$ joint torque feedback approach is proposed which takes into account the actuator's finite bandwidth dynamics, and minimizes the system's sensitivity to load torque disturbances and load dynamics. We also address implementation issues such as the development of a hydraulic dynamometer testbed for measurement of the disturbance sensitivity and of an innovative method for identifying the actuator dynamics. Experiment results with our experimental direct-drive motor demonstrate that the additional $\mathcal{H}^\infty$ positive torque feedback remarkably improves the disturbance attenuation and load decoupling properties of a simple PID motion controller. The optimal torque feedback also reduces the tracking error when dealing with a dynamic load while, unlike the conventional unity joint torque feedback, maintaining robust stability.**

***Index Terms*—Direct drive motors, disturbance rejection, H^∞ control, motion control, positive joint torque feedback (JTF).**

NOMENCLATURE

$C(s)$	motion controller transfer function (t.f.)
$G(s)$	torque disturbance t.f. of the motion controller
$G^+(s)$	torque disturbance t.f. of JTF
$G^+_{un}(s)$	torque disturbance t.f. of unity gain JTF
$G^+_{op}(s)$	torque disturbance t.f. of optimal JTF
$H(s), \hat{H}(s)$	actual, nominal actuator t.f.
j	$\sqrt{-1}$
$M(s)$	actuator rotor t.f.
$Q(s), Q_{op}(s)$	torque feedback, optimal torque feedback
$S(s)$	motion controller sensitivity function
$T(s)$	complementary sensitivity function of the motion controller
u, u^+	control input, compensated control input
$w_H(s)$	actuator uncertainty
$w_P(s)$	plant perturbation
$\Lambda(s)$	rotor-load transfer function
θ	actuator angle
τ_d, τ_s	driving torque, disturbance torque
$\chi(s)$	sensitivity function of JTF
$\chi^+(s)$	weighted sensitivity function of JTF
$\lvert\cdot\rvert$	absolute value of a complex number
$\lVert\cdot\rVert_\infty$	infinity norm of a transfer function

Manuscript received July 3, 2000. Manuscript received in final form February 26, 2001. Recommended by Associate Editor F. Ghorbel. This work was supported in part by the PRECARN TDS Project, through MPB Technologies of Montréal, QC, Canada.

F. Aghili is with the Canadian Space Agency, Space Technologies, Spacecraft Engineering, Saint-Hubert, QC, Canada (e-mail: farhad.aghili@space.gc.ca).

M. Buehler is with the Department of Mechanical Engineering, McGill University, Montreal, QC, Canada (e-mail: buehler@cim.mcgill.ca).

J. M. Hollerbach is with the Department of Computer Science, University of Utah, Salt Lake City, UT 84112 USA (e-mail: jmh@cs.utah.edu).

Publisher Item Identifier S 1063-6536(01)04941-7.

I. INTRODUCTION

THE need for high-performance motion control is pervasive in industrial applications, for example in automation, high-speed tracking and pointing systems, CNC machine tools [7], welding, laser cutting, or robotics. These high-performance motion control systems require accurate command tracking and good disturbance rejection. In general, it is understood that feedback control leads to a tradeoff between these requirements [14] because the disturbance cannot be attenuated without a measurement of its effect upon the system output. Torque disturbances can be either deterministic or random. For the deterministic case, such as free space motions of robotic manipulators, model-based controller can compensate the nonlinear load dynamics [8], [20]. However, model-based controllers are limited by parameter errors, structural modeling errors, parameter time variations, or simply unmodeled dynamics. There are also many application where the load torque cannot be predicted by a deterministic model, such as the cutting forces in a machine tool, or the wind forces in a tracking antenna. In these applications, high performance implies the ability of the control system to reject external torque disturbances.

Positive joint torque feedback (JTF)[1] can, in theory, be used to eliminate completely the effect of external torque disturbances and load torques on the motion servo. This requires that the system be endowed with built-in torque sensing which measures the load torque that is then precompensated via an ideal source of torque [1], [17], [15]. While the use of (high gain) negative joint torque feedback for purposes of actuator dynamics compensation has a long history [9], [11], [24], [18], positive joint torque feedback was proposed more recently. Kosuge [17] demonstrated experimentally the effectiveness of positive joint torque feedback to compensate the entire link dynamics of a SCARA-type direct-drive robot. The actuator dynamics was ignored and a simple control law with good robustness against varying loads was proposed. In this case, robot's link dynamics is completely decoupled and the remaining dynamics is the rotor dynamics which has been derived in our previous related work [1]. Hashimoto [15]

[1]This term is consistent with previous authors. However, the scheme can be treated as a feedforward as well.

applied this technique to an actuator geared with a harmonic drive where the deformation of the "flex-spline" is used to measure joint torque. The dynamic coupling terms in the robot dynamics are claimed to be small due to the high angular velocity of the rotors in comparison to that of the links, and therefore were treated as small disturbances. A survey of joint torque feedback can be found in [21].

Ideally, positive joint torque feedback with unity gain decouples the load dynamics exactly and provides infinite stiffness for external torque disturbance. This is because the torque feedback trivially compensated as an ideal actuator reproduces the same torque. However, the problem which stands in the way of compensating the load torques exactly is the actuator dynamics (which in the sequel is understood to include the servo amplifier dynamics as well as feedback loop delay) which has a finite bandwidth and therefore may not respond fast enough to the load torque. As a result, a complete compensation of disturbance torque or complete decoupling of load dynamics cannot be achieved in the presence of actuator dynamics. This can deteriorate the performance of the motion control system and even lead to instability. This is demonstrated in this paper via experimental results. The central contribution of this work is the formulation and design of positive joint torque feedback by taking the actuator's dynamics and uncertainty into account. Our strategy in the design of torque feedback, then, is to minimize the effect of load perturbation or of external torque disturbance. To this end, we seek an optimal filter for positive joint torque feedback control which takes the actuator's dynamics into account and minimizes, in the $\mathcal{H}^\infty$ sense, the sensitivity to load torque disturbance. We show that finding optimal torque feedback is equivalent to the model-matching problem [12], [13] that has an exact solution.

Often the load torques are generated by a dynamical system, as is the case in robot manipulators. In this case, we derive the entire system transfer function, under torque feedback. We show that the effect of the load dynamics enters as a perturbation to the nominal system, comprised of rotor and actuator dynamics. The optimal torque feedback minimizes the perturbation, makes the actual system close to the nominal system, and yields optimal robust stability when the motion controller deals with an uncertain load. It is important to note that the design of $\mathcal{H}^\infty$ position feedback for motion control is well known and has successfully been applied for some applications [22], [19] where the design is based on a nominal model comprised of actuator and load dynamics. In this paper, we introduce the design of positive feedback in the framework of $\mathcal{H}^\infty$ to optimally compensate the effect of load dynamics while the nominal model dynamics becomes the dynamics of the actuator's rotor to be controlled effectively by a simple feedback loop. We also present a novel method based on the measurement of disturbance sensitivity for the identification of the actuator dynamics on which the optimal control is based.

Accurate joint torque measurements encounter several design challenges. We developed a torque sensor prototype used herein that can measure joint torque accurately even in the presence of strong overhang forces and bending moments [6], [2].

This paper is organized as follows. Section II analyzes the inherent limitation of feedback control to attenuate load torque disturbances in motion servo mechanisms. This fact justifies the use of joint torque feedback in motion servo controllers where the servo mechanism is exposed to external disturbances. Section III is the main contribution of this work. Depending whether or not load torque is dynamic, there are two different solutions to the optimal torque feedback problem. If the torque disturbance is not correlated with the output, optimal joint torque feedback maximizes disturbance attenuation of a motion control system (Section III-B). In the case of dynamic load, optimal torque feedback minimizes the effect of load perturbation on the nominal rotor dynamics (Section III-C). Alternatively, the torque feedback can be optimally designed to achieve robust stability. Section III-E reformulates and solves the problem of an optimal torque filter to comply with model uncertainty and maximum filter gain specifications. Section IV extends the analytical results for the multivariable case. Implementation issues are addressed in Section V where we describe the development of a hydraulic dynamometer testbed to measure the disturbance sensitivity of a motion control system. A direct-drive motor integrated with torque sensor is also described briefly. Furthermore, we introduce a new method for indentification of acuator dynamics upon disturbance sensitivity of the system corresponding to two different torque feedback laws. Finally, Section VI evaluates the performance of the proposed torque feedback on our prototype when the motion control system deals with random disturbance or dynamic loads. The experimental results validate the developed theory and demonstrate the superior performance of our optimal torque feedback over conventional torque feedback.

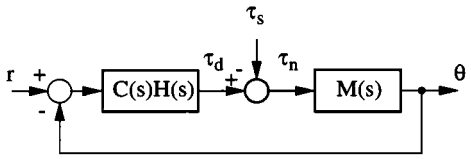

Fig. 1. A typical motion control system.

II. Feedback Limitation in Disturbance Attenuation

The general block diagram for a motion servo loop is shown in Fig. 1 where the controller $C(s)$ is cascaded with the plant $P(s) = H(s)M(s)$, comprised of the actuator $H(s)$, and the mechanical system $M(s)$. Usually, the actuator dynamics $H(s)$ is not considered in the design of motion controllers, since $M(s)$ is the dominant dynamics. Let θ be the actuator angle which should track the reference input r in the presence of external torque disturbances, τ_s. $\tau_n(s)$ is the net torque acting on the mechanical system

$$\tau_n(s) = \tau_d(s) - \tau_s(s) \tag{1}$$

where $\tau_d(s)$ denotes the torque developed by the actuator with the transfer function $H(s)$,

$$\tau_d(s) = H(s)C(s)[r(s) - \theta(s)] \tag{2}$$

and

$$\theta(s) = M(s)\tau_n(s). \tag{3}$$

The input-output (I/O) behavior of the closed-loop system is described by

$$\theta = [T(s) \quad G(s)] \begin{bmatrix} r \\ \tau_s \end{bmatrix} \tag{4}$$

where $T(s)$ and $G(s)$ show how the set-point and disturbance signals are transmitted to the system output at different frequencies. The transfer functions are related to the so-called sensitivity transfer function, $S(s)$, by $T(s) = 1 - S(s)$ called complementary sensitivity transfer function, and

$$G(s) = -S(s)M(s) = -\frac{T(s)}{C(s)H(s)} \tag{5}$$

where

$$S(s) = [1 + L(s)]^{-1} \tag{6}$$

and $L(s) = C(s)H(s)M(s)$ is the open-loop transfer function.

The primary concern in the design of the feedback transfer function $C(s)$ is to achieve or maintain stability of the closed-loop system. Additional performance requirements can be a specified tracking bandwidth, ω_c, and disturbance rejection over a certain frequency range. However, there is a conflict between these two requirements. Specifically, the feedback system in Fig. 1 is not able to attenuate external force disturbances over all frequencies within the closed-loop bandwidth. Since $H(s)$ and $M(s)$ are proper transfer functions, as they do not have any response at infinite frequency, and the causal controller $C(s)$ is at least a strictly proper transfer function, then the minimum relative degree of the open-loop transfer function must be two. Moreover, since $P(s) = H(s)M(s)$ is a stable plant, we can apply the Bode sensitivity integral [12]

$$\int_0^\infty \ln|S(j\omega)|\mathrm{d}\omega = 0. \tag{7}$$

In motion control systems, inertia dominates the plant dynamics M which is typically a double integrator. Hence, the magnitude of $M(j\omega)$ rolls off at high frequency. Moreover, as shown, L has a higher degree than M. Consequently, $|L(j\omega)|$ must roll off even faster than $|M(j\omega)|$. As a result, $|S(j\omega)|$ is close to 1 at frequencies sufficiently beyond the cutoff frequency ω_c. Equation (5) shows that $|G(j\omega)| = |S(j\omega)||M(j\omega)|$ leading to the following approximate relationship:

$$|G(j\omega)| \approx |M(j\omega)| \quad \text{for } |S| \approx 1 \text{ at } \omega > \omega_c. \tag{8}$$

By splitting the interval of the integrals in (7) into two subintervals as $\int_0^\infty \cdots = \int_0^{\omega_c} \cdots + \int_{\omega_c}^\infty \cdots$ and considering (8)

$$\int_0^{\omega_c} \ln|G(j\omega)|\mathrm{d}\omega \approx \int_0^{\omega_c} \ln|\mathrm{M(j\omega)}|\mathrm{d}\omega = \text{constant}. \tag{9}$$

Equation (9) reveals that there is little room to improve the disturbance sensitivity $G(j\omega)$ within the system bandwidth by design. In fact, any attempt to decrease the disturbance sensitivity over some frequency range amplifies inevitably the magnitude over the remainder of the bandwidth. As an illustration of this fact consider the plant dynamics as a double integrator for a simple mechanical system $M(s) = 1/(Js^2)$, where J is rotor polar inertia. Then the right-hand side (RHS) of (9) can be carried out in terms of an arbitrary bandwidth ω_c as

$$\mathrm{RHS} = \omega_\mathrm{c}\left(2 - \ln\left(\mathrm{J}\omega_\mathrm{c}^2\right)\right). \tag{10}$$

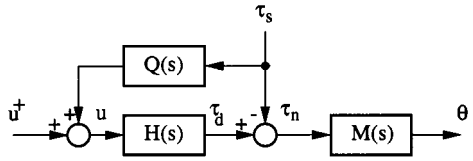

Fig. 2. Positive JTF system.

The minimum of maximum disturbance sensitivity is achieved when the disturbance sensitivity function is flat over the bandwidth $(0, \omega_c]$, i.e., for an optimal solution we have $\ln|G(j\omega)| = 2 - \ln(J\omega_c^2) = \text{constant}$. Therefore,

$$\min_{C(jw)} \|G(j\omega)\|_\infty \approx \frac{7.389}{J\omega_c^2} \quad \text{for } 0 < \omega < \omega_c. \tag{11}$$

The right-hand side of (11) decreases monotonically with ω_c. This implies that the higher the system bandwidth, the lower the magnitude of the disturbance transfer function. However, the maximum admissible bandwidth is restricted by the physical capability of the actuator. Therefore, it can be concluded that the minimum achievable $|G(j\omega)|$ within the bandwidth over all controllers is merely determined by the system inertia.

III. $\mathcal{H}^\infty$ Positive JTF

In this section we formulate JTF in the presence of actuator dynamics and seek a dynamical torque feedback to minimize external torque disturbance or to minimize effect of load perturbation. A single variable case is considered herein, yet the analytic solution will be extended for a multivariable case in Section IV.

A. Model-Matching Formulation

In the following, we examine the ability of the control system under positive joint torque feedback to eliminate the effect of disturbance. The general block diagram is shown in Fig. 2. The external disturbance τ_s is measured via a torque sensor between the rotor and the load and is fed back for compensation through a filter $Q(s)$.

Let $u(s)$ be the actuator input. We introduce a new input

$$u^+(s) = u(s) - Q(s)\tau_s(s) \tag{12}$$

which is the compensated control input under positive JTF. Now define the disturbance sensitivity function

$$\chi(s) \triangleq \frac{\tau_n(s)}{\tau_s(s)} = -1 + H(s)Q(s) \tag{13}$$

which shows how the disturbance torque τ_s is transmitted into the system—note that $\chi = -1$ in the absence of feedback. Our criterion to design the filter $Q(j\omega)$ is to minimize the worst-case transmissivity of the disturbance, i.e., $\|\chi(s)\|_\infty$, that is we seek an optimal filter in the sense of $\mathcal{H}^\infty$. Typically, a physical system like an actuator is strictly proper because it does not have any response at infinite frequency, $H(j\infty) = 0$, and hence $\chi(j\infty) = -1$. This implies that the disturbance attenuation by positive torque feedback may not be achieved if the frequency is not restricted. Indeed, the argument of the min–max problem is one, and by selecting trivially $Q(s) = 0$ the minimum ∞ norm is achieved. This implies that the

disturbance sensitivity may get worse by any kind of torque feedback if the frequency is not restricted.

Let $W_1(s) \in \mathcal{H}^\infty$ be a weighting function that shapes the disturbance gain over frequency

$$\chi_W(s) = W_1(s)\chi(s). \tag{14}$$

Note that $|W_1(s)|$ should roll-off at high frequency where $|\chi(s)| \approx 1$. Since the torque feedback is not able to attenuate high-frequency disturbances, $W_1(s)$ is used to determine the frequency band of interest. Furthermore, the maximum gain of $W_1(s)$ plays no role in finding the optimal Q, because it can be always be factorized in (14). Hence, for convenience we normalize $W_1(s)$ such that $||W_1(s)||_\infty = 1$. Let μ represent the maximum disturbance corresponding to an arbitrary filter $Q(s)$, i.e., $\mu = ||\chi_W||_\infty$. Now, the problem is to find a stable and realizable filter $Q(s) \in \mathcal{RH}^\infty$ ($\mathcal{RH}^\infty$ denotes the class of $\mathcal{H}^\infty$ functions which are rational) such that the maximum weighted sensitivity of the system is minimized, that is formulated mathematically

$$\mu_{\text{op}} = \inf_{Q(s)\in\mathcal{RH}^\infty} \sup_{\text{Re } s>0} |W_1(s)(1 - H(s)Q(s))| \tag{15}$$

where $\mu_{\text{op}} \leq \mu$. This is a model-matching problem, and algorithms to compute the optimal $Q_{\text{op}}(s)$ are readily available [12], [13].

How much can the disturbance sensitivity be reduced by joint torque feedback? Suppose μ is the maximum disturbance sensitivity corresponding to an arbitrary filter $Q(s)$. Hankel operation is an elegant solution for the maximum attainable attenuation on the disturbance, μ_{op}. The attenuation which determines the efficiency of the torque feedback method completely depends on the location of right half-plane zeros of the actuator transfer function $H(s)$. For a minimum phase system the solution is trivial and the disturbances can be attenuated at will. But when $H(s)$ has a single zero in the right half-plane s_0, $\text{Re } s_0 > 0$, according to the maximum modulus theorem [12] we can say $\mu_{\text{op}} \geq |W_1(s_0)|$ and $Q(s)$ has a unique solution. Since usually $W_1(s)$ is typically a low-pass behaved function, it can be concluded, in general, that the right half-plane zero near the origin adversely restricts the functionality of joint torque feedback. In other words, the location of actuator right half-plane zeros is a rough indication of the frequency range of the disturbance rejection which can be achieved by any torque feedback. A suitable choice of the weight function depends on the application, which is addressed in the sequel.

B. Optimal Disturbance Attenuation

In applications with significant external torque disturbances (e.g., machine tools for metal cutting, slow robots for contour grinding, precision index machines, or tracking radar antennas) disturbance attenuation is critical. Therefore, it is reasonable to define the disturbance sensitivity G^+ which describes the input τ_s to output θ relationship in the frequency domain. This is equivalent to the previous model-matching problem (15), if $M(s)$ is chosen as the weight function $W_1(s)$. However $M(s) \notin \mathcal{H}^\infty$ because $M(s)$ is unbounded at zero frequency, and hence there is no optimal solution if $W_1(s) = M(s)$. Next we investigate the disturbance attenuation with combined torque and position feedback, that is $u^+(s)$ is dictated by a position feedback.

Theorem 1: The maximum magnitude of the disturbance transfer function of a position control system combined with positive torque feedback is minimized, when the torque feedback filter $Q(s)$ is the model-matching solution of the weighted disturbance sensitivity in (15) where the magnitude of the weighting function is chosen as that of the normalized disturbance transfer function of position feedback, $|W_1| = |G|/||G||_\infty$.

Proof: Equation (13) shows how the external disturbance is transmitted into the control system with positive joint torque feedback. In this case the system output is

$$\begin{aligned}\theta =& M(s)[\chi(s)\tau_s + u^+] \\ =& M(s)\chi(s)\tau_s + M(s)H(s)C(s)[r - \theta] \\ =& G^+(s)\tau_s + T(s)r\end{aligned}$$

where G^+ is disturbance transfer function of the motion control system with positive torque feedback defined as

$$G^+(s) \triangleq G(s)[1 - H(s)Q(s)]. \tag{16}$$

Therefore

$$\begin{aligned}|G^+(s)| =& |G(s)\chi(s)| \\ =& ||G(s)||_\infty |\chi_W(s)|.\end{aligned} \tag{17}$$

In the above, χ_W is the weighted sensitivity where the weight function is chosen as $|W_1(s)| = |G|/||G||_\infty$. Since $\mu \leq \mu_{\text{op}}$, and knowing that $||G^+||_\infty = \mu||G||_\infty$, we can say

$$||G^+_{\text{op}}||_\infty \leq ||G^+||_\infty.$$

Therefore, the optimal torque feedback $Q_{\text{op}}(s)$ is the solution of the model-matching problem in (15) where the weight function $W_1(s)$ is chosen as the normalized position disturbance sensitivity $G(s)$.

It is worth noting that the disturbance sensitivity of the position feedback, $G(s)$, has a large amplitude at low frequency and decreases with frequency. Conversely, the magnitude of $\chi(s)$ is small at low frequency and it increases with frequency. Therefore, it can be concluded from (16) that the combined position and torque feedback makes disturbance attenuation over a wide frequency range feasible.

C. Optimal Robust Stability for Dynamic Load

The above optimal positive torque feedback is well suited for systems in which no correlation exists between the torque disturbance τ_s and the system output θ. However, for industrial applications such as in robotics, τ_s is produced by the load dynamics, and there is a dynamical relationship between the disturbance torque, τ_s, and net torque, τ_n. We assume that the structure of the load dynamics is unknown, leading to an uncertain dynamical relationship between τ_n and τ_s. This means there is no nominal dynamical model defined for the load. However, the maximum bound over the ratio of the two signals at each frequency is assumed known. The formal way to represent that uncertainty mathematically is

$$\frac{\tau_s}{\tau_n} = \Lambda(jw)\Delta, \quad \forall|\Delta| \leq 1, \ \forall\omega \tag{18}$$

where Δ is any transfer function which at any frequency is less than one. $\Lambda(s)$ is a rational transfer function ("rotor-load" transfer function) whose magnitude envelopes the ratio of the

two signals. Our strategy then is to minimize the effect of the load dynamics perturbation. Note that, since $\Lambda(s)$ is the I/O representation of a physical system, it is reasonable to assume that it is bounded.

Now, we show that the effect of the load dynamics on a system with JTF enters in the form of an inverse-multiplicative perturbation to the nominal plant $P(s) = M(s)H(s)$. Referring to Fig. 2 and (18) we obtain

$$\tau_n = H(s)u^+ + \chi(s)\tau_s. \tag{19}$$

By replacing τ_s in the above from (18)

$$[1 - \chi(s)\Lambda(s)\Delta]\tau_n = H(s)u^+. \tag{20}$$

Finally, multiplying the both sides of (20) by $M(s)$, and using $P = MH$

$$\frac{\theta}{u^+} = [1 - w_P(s)\Delta]^{-1}P(s), \quad \forall|\Delta| < 1 \tag{21}$$

where $w_P(s)$ is defined as

$$w_P(s) = \chi(s)\Lambda(s). \tag{22}$$

Equation (21) describes a perturbed system in which $w_P(s)\Delta$ enters as a inverse-multiplicative perturbation to the nominal plant $P(s)$. The worst-case magnitude of the perturbation occurs when $|\Delta| = 1$, hence we have

$$|w_P| = |\chi'_W|||\Lambda||_\infty \tag{23}$$

where the weight function, analogous to the previous section, is chosen as $|W_1(s)| = |\Lambda(s)|/||\Lambda(s)||_\infty$. Hence $||w_p||_\infty = \mu'||\Lambda||_\infty$, where $\mu' = ||\chi'_W||_\infty$. Note that $||\Lambda||_\infty$ is the maximum magnitude of the rotor-load transfer function which is independent of the control. μ' is the maximum weighted disturbance sensitivity that can be minimized by the optimal torque feedback (15). Moreover, since P is stable, the condition for robust stability of the nominal open-loop transfer (21) is that $|1 - w_P(s)\Delta| > 0$. This condition can be satisfied if

$$\mu'||\Lambda||_\infty < 1. \tag{24}$$

The load perturbation is minimum by applying the optimal filter Q_{op} which minimizes μ'. That is equivalent to solve the model-matching problem when the weight function is chosen as $|W_1(s)| = |\Lambda(s)|/||\Lambda(s)||_\infty$. Hence, the design requires an envelope of the magnitude-frequency of the τ_n to τ_s transfer functions which are load dependent. To this end, $|\Lambda|$ can be approximated by any transfer function whose magnitude envelopes all empirical transfer functions representing different load case scenarios obtained from experiments. This will be described in Section V-D.

Alternatively, the torque feedback can be designed to achieve optimal robustness of the motion control system. Assuming that the perturbed open-loop transfer function $L_P(s) = [1 - w_p(s)\Delta]^{-1}L(s)$ is stable, i.e., $|w_P(s)| < 1$, and assuming stability of the nominal closed-loop system, it follows that $S(s)$ is a stable transfer function. The Nyquist criterion specifies that the robust stability is then guaranteed if encirclements by $L_P(s)$ of the point -1 are avoided, or

$$|1 + (1 - w_P(s)\Delta)^{-1}L(s)| > 0, \quad \forall|\Delta| < 1, \ \forall\omega. \tag{25}$$

Since $1 + w_P(s)\Delta$ is always positive, it can be multiplied to the left-hand side of the above inequality. Moreover, considering the worst-case $|\Delta| = 1$, we have the robust stability condition as

$$\begin{aligned} \text{RS} &\Leftrightarrow |1 - w_P + L| > 0 \quad \forall\omega \\ &\Leftrightarrow |1 + L| - |w_P| > 0 \\ &\Leftrightarrow |Sw_P| = |\chi''_W|||S\Lambda||_\infty < 1 \end{aligned}$$

where the corresponding weight function is chosen as $|W_1(s)| = |S\Lambda|/||S\Lambda||_\infty$ for χ''_W, and $\mu'' = ||\chi''_W||_\infty$. Then the above condition for robust stability can be written as

$$\mu''||S\Lambda||_\infty < 1. \tag{26}$$

In summary, optimal robust stability of the closed-loop motion control system with positive JTF can be achieved if the torque filter is the solution of the model-matching formulation with the weight function $|W_1(s)| = |S\Lambda|/||S\Lambda||_\infty$.

Since the nominal open-loop system $L(s)$ is stable, we have $|S| < 1$, and $\mu' > \mu''$—note that $|\chi''_W| = |S||\chi'_W|$. This implies that the earlier condition (24) is more conservative than the latter one (26). Indeed, in (21), we attempted to minimize $|w_P(s)|$ uniformly over all frequencies by the positive JTF. Nevertheless, the condition in (26) implies that to achieve optimal robustness performance of the closed-loop system, $w_P(s)$ must be minimized at frequencies where $S(s)$ is large.

It is also important to note that, inequality (26) implies that either low attenuation of the weighted disturbance μ'' or heavy load, i.e., high $|\Lambda|$, can potentially lead to instability. Yet, in practice, μ'' is substantially reduced by optimal JTF providing robust stability. Roughly speaking, $||\Lambda(s)||$ increases by increasing the ratio of the rotor to load inertia. Therefore, the robust stability of the motion control system with positive JTF deteriorates with heavy loads.

D. Selecting the Weighting Function

The purpose of the weighting function $W_1(s)$ is to shape the power spectrum density of the JTF disturbance function $\chi(s)$. Therefore, only the magnitude $|W_1(j\omega)|$ of the weighting function plays a role, not the phase. The last two sections suggest how the weighting function $W_1(s)$ should be selected. In general, a suitable choice of the weight function depends on the application and can be selected as follows:

1) $|W_1| = |G|/||G||_\infty$ minimizes torque disturbance sensitivity,
2) $|W_1| = |\Lambda|/||\Lambda||_\infty$ minimizes the perturbation of a dynamic load,
3) $|W_1| = |S\Lambda|/||S\Lambda||_\infty$ yields optimal robust stability when dealing with a dynamic load.

E. Two-Block $\mathcal{H}^\infty$ Formulation

The JTF approach described so far requires an actuator transfer function. However, in most real-world systems, at high frequencies the structure and model order of the actuator is unknown. Since the plant dynamics at high frequency can be very complex and/or nonlinear, it is preferable to work with a simpler plant model approximation to reduce the order of controller. The worst-case deviation from the nominal dynamics is represented by the ∞—norm of the "model uncertainty" which underlies the subsequent JTF development.

Suppose the real actuator torque dynamics H is described in the form of a multiplicative uncertainty, $H = \hat{H}(1 + w_H\Delta')$ where the nominal transfer function $\hat{H}(s)$ is accompanied by the uncertainty Δ' that can be any transfer function provided $|\Delta'(j\omega)| \leq 1$. Then, the optimization problem leading to the solution of $Q_{\rm op}(s)$ in the presence of actuator modeling uncertainty is

$$\begin{aligned}\mu_{\rm op} &= \inf_{Q(s)\in\mathcal{RH}^\infty} \sup_{|\Delta'(s)|\leq 1} \sup_{\mathrm{Re}\, s>0} \left|W_1(1-\hat{H}Q) + W_1\hat{H}w_H\Delta'Q\right| \\ &\leq \sqrt{2} \inf_{Q(s)\in\mathcal{RH}^\infty} \sup_{\mathrm{Re}\, s>0} \left\|\begin{bmatrix} W_1(1-\hat{H}Q) \\ W_2Q \end{bmatrix}\right\|_\infty \end{aligned} \tag{27}$$

where

$$W_2 = W_1\hat{H}w_H. \tag{28}$$

Therefore, we reformulate our original problem (15) in the *two block form* (27) from which an optimal feedback can be obtained. To solve this problem, one can be transform (27) into the standard model-matching problem by changing variables as described in Appendix I.

Some interesting observations can be made at this point. Due to its simplicity, our model-matching $\mathcal{H}^\infty$ JTF formulation does not allow any specifications for the torque filter $Q(s)$. Nevertheless, the magnitude of the torque filter $Q(s)$ should roll off at high frequencies. The torque response resembles a low-pass filter which makes a high-pass behaved optimal torque filter because, roughly speaking, the solution of the model-matching problem is equivalent to inverting a given transfer function. Consequently, in practice, the amplitude of the torque filter $Q(s)$ increases unboundedly at high frequency. The high gain produces a large control effort which causes overheating of the power amplifier and the actuator. Therefore, it is reasonable to roll off the torque feedback at high frequency where the magnitude of $G(j\omega)$ is sufficiently low. On the other hand, it can be inferred from (27) that since the optimization procedure suppresses the infinity norm of $|W_2(s)Q(s)|$, the magnitude of the torque filter Q is shaped by the magnitude-frequency of the second weight function W_2. Since $|w_P(s)|$ is almost zero at low frequencies, W_2 reassembles a high-pass behaved system penalizing the magnitude of the torque feedback at high frequency. This causes the magnitude of the torque filter $Q(s)$ is rolled off at high frequency. Nevertheless, the torque feedback is redundant at high frequencies where the inertia of the system naturally attenuates torque disturbances.

IV. The Multivariable Case

So far we have considered single joint system. Yet, the analytical results can be extended for a multivariable case, applicable to robot manipulators. It has been shown [1] that the coupled rotor dynamics of an n joint manipulator can be represented by

$$\mathbf{M}(s) = \frac{1}{s^2}(\mathbf{I}+\mathbf{D})^{-1}\mathbf{J}_p^{-1} \in \mathbb{R}^{n\times n} \tag{29}$$

where

- $\mathbf{J}_p$ diagonal matrix whose elements are the polar inertias of the joint's motors;
- $\mathbf{I}$ identity matrix;
- $\mathbf{D}$ is a strictly upper triangular matrix whose elements are dependent of the robot's twist angles (refer to [1] for more details).

In addition, let $\mathbf{G}(s) \in \mathbb{R}^{n\times n}$ represent the multivariable disturbance sensitivity function corresponding to the plant $\mathbf{M}(s)$ and the position controller $\mathbf{C}(s)$. $\mathbf{G}^+(s) \in \mathbb{R}^{n\times n}$ represents the torque disturbance sensitivity under composite position and torque feedback loops in the same fashion as defined for the single variable case. Also, suppose $\mathbf{Q}(s) \in \mathbb{R}^{n\times n}$ is a matrix corresponding to a multichannel joint torque feedback, and

$$\mathbf{H}(s) = \mathrm{diag}\,[H_1(s), H_2(s), \ldots, H_n(s)]$$

is a diagonal transfer function matrix representing the dynamics of the joint actuators. Analogously to the single output case, we attempt to minimize the worst-case weighted sensitivity function of positive torque feedback, i.e., $\chi_W = \mathbf{W}_1\chi$, by applying an optimal multichannel torque feedback. By using the definition of the infinity norm for multivariable transfer function and by using properties of singular value, we have

$$\|\chi_W\|_\infty \leq \sup_\omega \bar{\sigma}(\mathbf{W}_1(j\omega))\bar{\sigma}(\mathbf{I} - \mathbf{H}(j\omega)\mathbf{Q}(j\omega)) \tag{30}$$

where $\bar{\sigma}(\cdot)$ denotes the maximum singular value of a matrix via $\bar{\sigma}(\mathbf{A}(s)) = \sqrt{\lambda_{\max}(\mathbf{A}(-s)\mathbf{A}(s))}$, and $\lambda_{\max}(\cdot)$ is the maximum eigenvalue. Equation (30) involves solving a multivariable model-matching problem. In general this is a challenging analytical problem [13]. Yet, in this case, the optimal solution $\mathbf{Q}_{\rm op}$ has a diagonal form like the actuator transfer function matrix. By virtue of the Lemma given in Appendix II, one can show that the optimal form of the second term on the RHS of (30) must be in a diagonal form. Therefore, the optimal torque filter in (30) must be decoupled, i.e., $\mathbf{Q}(s)$ is a diagonal matrix. This reduces the multivariable $\mathcal{H}^\infty$ problem of the single-variable case, solved in the previous sections. Hence, the following holds for the RHS of (30):

$$\mathrm{RHS} \leq \inf_{\mathbf{Q}(s)\in\mathcal{RH}^\infty} \max_i \sup_\omega \bar{\sigma}(\mathbf{W}_1(j\omega))(1 - H_i(j\omega)Q_i(j\omega)) \tag{31}$$

suggesting that the design of JTF for each joint involves solving the single-variable model-matching problem where the scalar weight function is the singular value of the matrix weight function. Following the same arguments as for the single axis case, the weight function matrix is chosen depending on application described in Sections III-B and III-C.

V. Implementation Issues

This section describes the implementation of JTF for a single axis joint. To this end, a hydraulic dynamometer was built that allows us to measure the disturbance sensitivity of a motion control system. We also developed a novel procedure for the identification of the actuator dynamics based on disturbance sensitivity measurements. The ability of JTF to decouple the effect of load dynamics is assessed by using an arm whose counterbalance weight can be changed. An envelope over the rotor-load transfer function is obtained experimentally and is used to design the JTF.

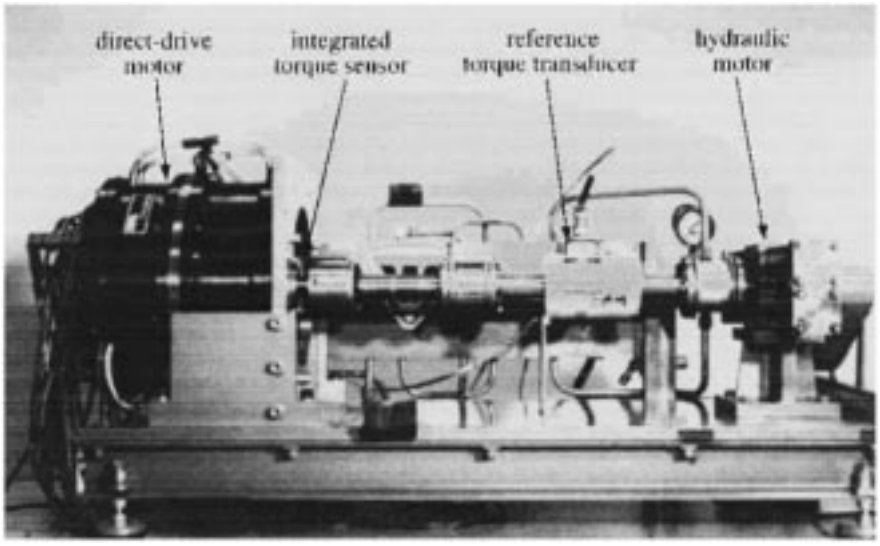

Fig. 3. Direct-drive motor on the hydraulic dynamometer testbed.

A. Hardware Description

Fig. 3 illustrates the experimental setup which consists of the McGill/MIT Direct-Drive electric motor [4], [16] mounted on the dynamometer, instrumented with our custom torque sensor [2], and coupled to a hydraulic rack and pinion rotary motor (Parker 113A129BME). The hydraulic motor's shaft is connected to the direct-drive motor by means of two couplings (Gam/Jakob KSS-450), via an additional commercial reference torque transducer. The role of the hydraulic motor is to generate a random disturbance torques. To achieve this goal, the solenoid-valve of the hydraulic motor is interfaced to computer by a binary high-voltage isolation amplifier, thereby a simple open-loop ON–OFF control is possible. The solenoid is activated by a random sequence generated by computer.

The system architecture is briefly described in the following. The analog torque signal is processed by antialiasing filters and digitized through a multichannel 16-bit A/D converter. Digital position data from a custom-built counter is read into the computer through the digital I/O port of the data acquisition board. The three desired phase current output commands, determined by a minimum ripple commutation law [5], [3], are converted to analog signals via D/A converters for the inputs to the power amplifiers which operate in current control mode (see Fig. 4.

The sixth-order optimal filter was converted to the z-domain equivalent via the Tustin transformation, and implemented on a 66-MHz 80 486–based IBM compatible microcomputer. The time to apply this $\mathcal{H}^\infty$ filter to the torques was only 13 μs, which is small compared to the 106 μs taken up by I/O tasks.

B. Position Controller

In the course of our experiments, it became evident that joint torque feedback introduces a bias in position tracking due to the torque sensor offset. Strain gauges are notorious for their sensitivity to temperature. Theoretically, it should not affect the Wheat-stone output because of symmetry. However, the gauges do not have identical characteristics and a bias voltage appears frequently. The sensor bias acts as a constant disturbance on the position controller resulting in a steady-state

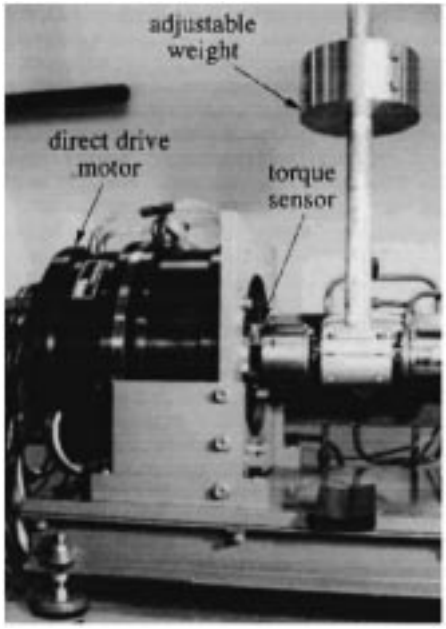

Fig. 4. The single joint direct drive system.

error. According to (5), the steady-state position error is $e_{\text{off}} = -\tau_{\text{off}} T(0)/H(0)C(0)$, where τ_{off} is the torque sensor offset. Since the complementary sensitivity must be one at zero frequency (due to the interpolation constraint for stability), $T(0) = 1$, and $H(0) = 1$, we have

$$e_{\text{off}} = -\frac{\tau_{\text{off}}}{C(0)}.$$

This offset is eliminated by the integral term in our PID position controller

$$C(s) = K_P + \frac{K_I}{s} + K_D s \tag{32}$$

where $C(0) = \infty$. In our application a PID position controller, $u^+ = K_P e + K_I \int e dt + K_D \dot{e}$, is used whose gains are tuned as the followings: $K_P = 40$ Nm/deg, $K_I = 200$ Nm/deg·s, and

$K_D = 0.8$ (Nm · s/deg). The bandwidth of the position servo with the corresponding gains is close to 10 Hz.

C. Identification of Actuator Dynamics

The performance of joint torque feedback critically relies on the knowledge of actuator dynamics—the larger the modeling uncertainty, the lower ability of JTF to suppress load torque. The first step in identification process involves the determination of the empirical (nonparametric) transfer function based on spectral analysis of the stochastic I/O signals [10]. Our early experiments to extract the torque frequency response based on a direct measurement of an actuator's I/O have not been successful. The main obstacle is the interference of mechanical dynamics, due to motion of rotor, that cannot be excluded even when the motor shaft is locked. The flexibility of the mechanical locking device and the torque transducer accompanied with the rotor inertia introduce a dynamical system cascaded with the torque dynamics. The dynamical system causes the observed torque signal being the filtered version of the actuator torque. Therefore, in order to identify the actuator's dynamics accurately, the stiffness should be high enough such that the modal frequency of mechanical system is at least ten times that of the actuator cutoff frequency. This is difficult to achieve in practice.

We used an alternative method to derive the torque transfer function accurately. The method is based on measurement of the disturbance sensitivities when different joint torque feedbacks are applied. Assume $G_{\text{un}}^{+}(\omega)$ denotes the disturbance transfer function under unity gain positive JTF, i.e., $Q = 1$. As will be shown in Section VI-A, the disturbance sensitivity test describes the amplitude and phase related frequency corresponding to $G_{\text{un}}^{+}(\omega)$ and $G(\omega)$. Then, by virtue of (16), one can obtain the empirical (nonparametric) transfer function $H(\omega)$ via

$$H(\omega) = 1 - \frac{G_{\text{un}}^{+}(\omega)}{G(\omega)}. \tag{33}$$

The next step of the identification involves a numerical procedure to represent the complex function (33) by a rational transfer function as close as possible. To this end, the coefficients of the numerator and denominator of a fixed order rational function were calculated to fit the complex frequency responses in the least squares sense. Several parametric models were examined, and it turned out that a second-order systems is sufficient to match the I/O behavior adequately. The empirical and parametric representation of the actuator dynamics is shown in Fig. 5 (top) which demonstrates graphically the validation of the parametric system model. The deviation of the parametric model from the actual system response can be measured quantitatively by

$$|w_H(j\omega)| \geq \left| \frac{H(\omega)}{\hat{H}(j\omega)} - 1 \right|. \tag{34}$$

Fig. 5 (bottom) shows the magnitude of the deviation. A conservative bound for the uncertainty is estimated by a first-order rational function $w_H(j\omega)$ which also extrapolates the uncertainty at high frequency where there is no experimental information. Recall from (27) that a conservative model for the structured uncertainty is required to synthesize the $\mathcal{H}^{\infty}$ joint torque feedback. The graph shows that the modeling uncertainty is growing with frequency.

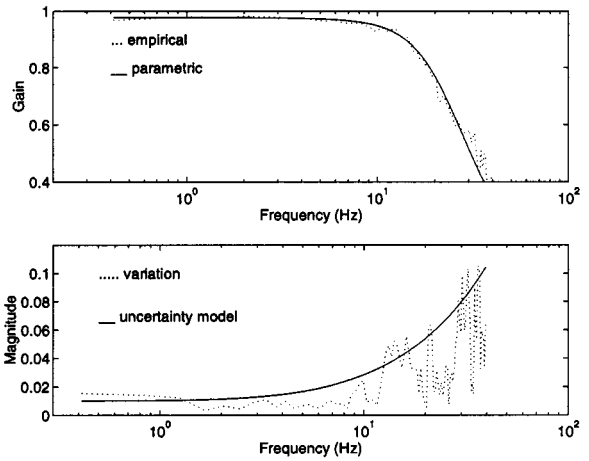

Fig. 5. Frequency responses of the actuator (top); dashed is $|H(\omega)|$ and solid is $|\hat{H}(j\omega)|$. Structured uncertainty (bottom); dashed is deviation from the nominal dynamics, $|H(\omega)/\hat{H}(j\omega)|$, and solid is uncertainty model by a first-order function $w_H(j\omega)$.

D. Rotor-Load Transfer Function

As discussed in Section III-C, in order to design the optimal torque feedback in the case of dynamic load, we need to know the worst-case magnitude of the net torque to sensor torque, represented by $|\Lambda(j\omega)|$. Similar to Section V-C, we performed spectral analysis of the stochastic I/O signals to determine the transfer function. The input signal is a small white noise signal added to the reference input that excites all mechanical modes. The control input signal u is known because it is issued by the computer, while the output signal is τ_s measured by the torque sensor. Suppose the empirical transfer function $Z(\omega)$ represents the control effort signal u to torque sensor signal τ_s. Then, the rotor-load transfer function can be reconstructed from $Z(\omega)$ by

$$|\Lambda(\omega)| \geq |H(\omega)Z(\omega) - 1|^{-1}. \tag{35}$$

The magnitude of $|\Lambda|$ obtained from experiment is shown in Fig. 6 for two extreme loads corresponding to 0.7 kgm^2 and 1.9 kgm^2. The graphs show that the mechanical modal frequencies occur between 20 and 40 Hz, and the maximum amplification of the net torque to sensor torque is 12. The solid line shows a conservative envelope, used as the weight function $W_1(s)$ to design JTF. Note that a tighter envelope requires a higher order transfer function, leading to a more complex controller.

VI. Experimental Validation

This section evaluates the performance of the proposed JTF experimentally in terms of torque disturbance attenuation and position tracking accuracy under varying payload. In order to measure the torque disturbance sensitivity, torque disturbances are injected into the direct-drive system by the hydraulic dynamometer. An arm with adjustable payload is mounted on the motor's shaft to investigate the load decoupling and robust stability properties.

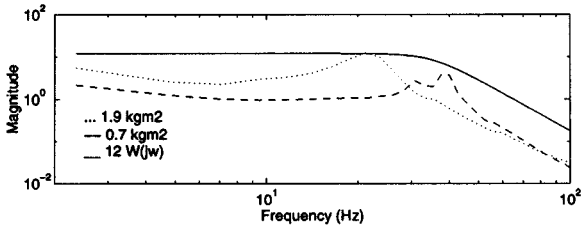

Fig. 6. Graph of $|\Lambda|$ with two load cases.

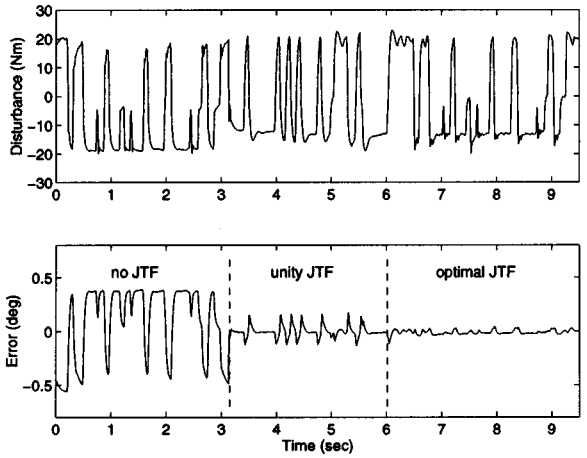

Fig. 7. Tracking error with different joint torque feedback.

A. Disturbance Attenuation Measurement

In this section, we compare the disturbance attenuation of conventional unity gain positive JTF with that of the proposed $\mathcal{H}^\infty$ JTF (Section III-B). To this end, we command a ramp reference signal through the PID position controller (Section V-B) while the hydraulic motor injects random torque disturbances. Fig. 7 shows applied the torque disturbances and the resulting position tracking errors for three different torque feedback laws. The system exhibits high disturbance sensitivity without any JTF. The conventional unity gain JTF is able to reject the slow varying part of torque disturbances, but is sensitive to the fast torque variation. The figure clearly shows that the tracking error is substantially reduced with $\mathcal{H}^\infty$ JTF.

Next, we perform a spectral analysis on the time series output–input data, to obtain the complex frequency response [23], disturbances transfer functions, shown in Fig. 8. As expected, the position servo system without torque feedback exhibits high sensitivity to disturbance within the loop bandwidth. It is also apparent that the system with the unity gain JTF, $Q(s) = 1$, performs better than without any JTF, especially at low frequencies. However, at higher frequencies there is little improvement. This can be explained by the low-pass characteristics of the actuator dynamics. At low frequencies where the actuator dynamics are negligible, it is able to produce exactly the required torque. However, at higher frequencies the produced torque appears in different amplitude and phase from that of torque disturbance depending upon actuator dynamics. Thus the net torque increases with frequency and so does the disturbance sensitivity. Nevertheless, at sufficiently high frequency, the disturbance sensitivity drops again due to

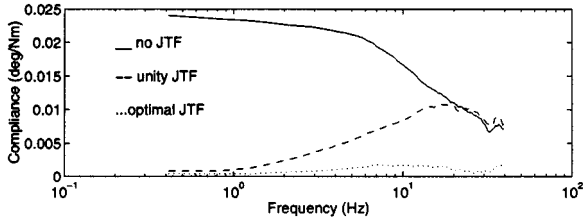

Fig. 8. Experimental disturbance attenuation with different JTF.

the attenuation effect of position feedback itself, because the position disturbance sensitivity weighs the torque feedback disturbance sensitivity. The unity gain JTF has its maximum disturbance sensitivity at 15 Hz with a relatively high peak value. As it shall be shown in the next section, this resonance can cause instability when the system encounters a dynamical load. The optimal feedback lowers the system sensitivity to disturbance remarkably over the whole frequency range. This validates the superior performance of the proposed JTF.

It is worth nothing that, since the actuator and position sensor are co-located, the joint angle is slightly different from the sensed angle. The difference is due to the compliance of the torque sensor. The sensor compliance has been measured experimentally to be 2.1×10^{-4} deg/Nm [2]. It is almost one order lower than the value of the controller compliance. This fact clarifies that any improvement on lowering the disturbance sensitivity lies on reducing the disturbance sensitivity of the motion controller rather on incorporating a stiffer torque sensor or compensating its effect.

B. Robustness Stability Under Dynamic Load

This section presents some results for robotics application where there exists a relationship between the load disturbance and the system output. The main objective is to investigate the performance and stability of positive joint torque feedback as derived in Section III-C, under dynamical load. To this end, a link with a 7.2 kg mass is mounted on the motor's torque sensor (Fig. 4). The mass plays the role of an uncertain payload. The weight can be mounted at different distances from the rotation axis to change the link's inertia and gravitational torque. The counterbalance weight produces a nonlinear gravity torque to be compensated with positive joint torque feedback. To investigate the tracking performance of the control system, we command a sinusoidal reference position trajectory $r(t) = 45 \sin 0.18t$ degrees to the PID controller.

First, no JTF is applied. Since the nonlinear link dynamics (due to the gravitational term) are not compensated by a JTF controller, the tracking error resulting from the PID controller alone is large, as shown in Fig. 9 (top). Next, we apply unity gain and the $\mathcal{H}^\infty$ JTF in addition to the PID position controller. As discussed earlier in Section III-C, the performance of JTF deteriorates with heavy loads as it produces a stronger disturbance torque. Thus, we chose the heavy load (1.9 kgm^2) for demonstration. Indeed, it turned out the optimal JTF has little merit over the conventional unity gain JTF for relatively light loads. However, with the heavy load, the conventional unity gain joint torque feedback exhibits unstable behavior as shown in Fig. 9 (middle). Yet, when the optimal joint torque feedback is applied

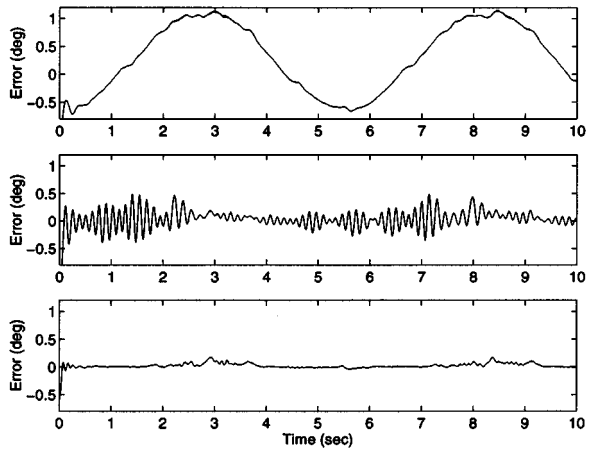

Fig. 9. Position tracking error trajectories with (top) no JTF, (middle) unity gain JTF, and (bottom) optimal JTF.

the tracking error is reduced significantly while maintaining stability, Fig. 9 (bottom).

VII. Conclusion

In this paper, we formulated the problem of optimal positive JTF in the presence of actuator's finite bandwidth dynamics to compensate the effect of load torque. We showed analytically and demonstrated experimentally, that the conventional unity gain torque feedback is not appropriate for the compensation. This is because in practice actuators and their power amplifiers have finite bandwidth and hence cannot respond fast enough to the load torque. We designed an $\mathcal{H}^\infty$ positive joint torque feedback which can optimally suppress the effect of load torque disturbance on a motion control systems in the presence of actuator dynamics.

The optimal torque feedback can be designed to minimize the magnitude of the disturbance sensitivity or to minimize the perturbation caused by a dynamic load. The theory of JTF based the framework of $\mathcal{H}^\infty$ was further developed to address uncertainty in the actuator model itself, and to solve the MIMO case as well.

An experimental setup comprised of a direct-drive electric motor, torque-sensor, and hydraulic motor was constructed to measure disturbance sensitivity of a motion servo mechanism. A novel method based on the measurement of disturbance sensitivity is also introduced for the identification of the actuator dynamics on which the optimal control is based.

To demonstrate the performance of the proposed torque feedback, a typical motion controller for the direct-drive motor was implemented while the torque disturbances were injected by a hydraulic motor. The performance of the joint torque feedback to decouple a dynamic load was also investigated by using a single link. The results demonstrated that the unity gain positive torque feedback has poor disturbance attenuation at high frequencies where the actuator dynamics becomes important. However, when the actuator was cascaded with the optimal filter, a significant reduction in sensitivity was achieved. In our second experiment, a single link with adjustable inertia was attached to the motor. In the absence of any torque feedback, the tracking error increased due to load nonlinearity, and increases with payload. Both conventional unity gain and $\mathcal{H}^\infty$ torque feedback substantially reduced the tracking error for small loads. However, the conventional unity gain torque feedback destabilizes the system for larger loads while the $\mathcal{H}^\infty$ feedback maintains stability and tracking accuracy.

Appendix I

Let $K_1(s) = W_1(s)H(s)$, and define the vector $\mathcal{T}(s)$ as

$$\mathcal{T} = \begin{bmatrix} W_1 - K_1 Q \\ W_2 Q \end{bmatrix}.$$

For a real valued function we have $|\mathcal{T}(s)|^2 = \tilde{\mathcal{T}}(s)\mathcal{T}(s)$ where $\tilde{\mathcal{T}}(s) = \mathcal{T}^{\mathrm{T}}(-s)$. The objective function to be minimized is $\mu^2 = \tilde{\mathcal{T}}(s)\mathcal{T}(s)$,

$$\begin{aligned}\tilde{\mathcal{T}}(s)\mathcal{T}(s) =& \tilde{W}_1 W_1 - \tilde{W}_1 K_1 Q - \tilde{Q}\tilde{K}_1 W_1 \\ &+ \tilde{Q}(\tilde{K}_1 K_1 + \tilde{W}_2 W_2) Q. \end{aligned} \tag{36}$$

For any positive semidefinite $G(s)$, the spectral factorization is defined as

$$G(s) = \tilde{G}_s(s) G_s(s) \quad G(s) \geq 0.$$

Now if $K(s)$ and $G(s)$ are defined as

$$\tilde{K}(s)K(s) = \tilde{K}_1(s)K_1(s) + \tilde{W}_2(s)W_2(s) \tag{37}$$

and

$$G(s) = \tilde{K}^{-1}(s)\tilde{K}_1(s)W_1(s), \tag{38}$$

one can show that the RHS of the following equation is positive semidefinite, therefore a spectral factorization exists, i.e.,

$$\tilde{R}(s)R(s) = \tilde{W}_1(s)W_1(s) - \tilde{G}(s)G(s). \tag{39}$$

Now by substituting $K_1(s)$, $W_1(s)$ and $W_2(s)$ from (37)–(39) into the RHS of (36), we have

$$\tilde{\mathcal{T}}(s)\mathcal{T}(s) = \tilde{G}G + \tilde{R}R - \tilde{G}KQ - \tilde{Q}\tilde{K}G + \tilde{Q}\tilde{K}KQ. \tag{40}$$

The RHS of (40) is equal to $\tilde{\mathcal{T}}'(s)\mathcal{T}'(s)$ where $\|\mathcal{T}(s)\|_\infty = \|\mathcal{T}'(s)\|_\infty$, and

$$\mathcal{T}'(s) = \begin{bmatrix} G(s) - K(s)Q(s) \\ R(s) \end{bmatrix}. \tag{41}$$

Since the second row in vector $\mathcal{T}'(s)$ does not depend upon $Q(s)$, the optimal solution underlies the solution of the standard model-matching problem in the first row of vector $\mathcal{T}'(s)$.

Appendix II

Lemma 1: Let $\mathbf{A}$ and $\mathbf{B}$ be square diagonal and nondiagonal matrices respectively, where $\mathbf{A}$ and $\mathbf{B}$ have identical diagonal elements. Then their maximum singular values are related as follows:

$$\bar{\sigma}(\mathbf{A}) \leq \bar{\sigma}(\mathbf{B}). \tag{42}$$

Proof: Suppose the mth element has the largest absolute value among all diagonal elements, hence

$$\bar{\sigma}(\mathbf{A}) = |a_{mm}| = |b_{mm}|. \tag{43}$$

By the definition of the infinity norm of matrices, we have

$$\bar{\sigma}(\mathbf{B}) = \|\mathbf{B}\|_\infty \geq \|\mathbf{B}\mathbf{x}\|_2 \quad \text{where } \mathbf{x} : \|\mathbf{x}\|_2 = 1. \tag{44}$$

Now choose all components of vector $\mathbf{x}$ in (44) zero except $x_m = 1$. Then

$$||\mathbf{Bx}||_2 = \left(|b_{1m}|^2 + |b_{2m}|^2 + \cdots + |b_{mm}|^2 + \cdots\right)^{1/2} \geq |b_{mm}|. \quad (45)$$

(42) can be concluded from (43)–(45).

REFERENCES

[1] F. Aghili, M. Buehler, and J. M. Hollerbach, "Dynamics and control of direct-drive robots with positive joint torque feedback," in *Proc. IEEE Int. Conf. Robot. Automat.*, Apr. 1997, pp. 1156–1161.

[2] ——, "A joint torque sensor for robots," in ASME Int. Mech. Eng. Congr. Exposition, Dallas, TX, Nov. 1997.

[3] ——, "Torque ripple minimization in direct-drive systems," in *Proc. IEEE/RSJ Int. Conf. Intell. Syst. Robots*, Victoria, BC, Canada, Oct. 1998, pp. 794–799.

[4] ——, "Development of a high-performance direct-drive joint," in Proc. IEEE/RSJ Int. Conf. Intell. Syst. Robots, Japan, Oct. 2000.

[5] ——, "Optimal commutation laws in the frequency domain for pm synchronous direct-drive motors," *IEEE Trans. Power Electron.*, vol. 15, pp. 1056–1064, 2000.

[6] ——, "Sensing the torque in a robot's joint," *ASME Mechanical Engineering, Feature Focus Article*, vol. 120, no. 9, pp. 66–69, Sept. 1998.

[7] A. G. Alsoy and Y. Koren, "Control of machine processes," *ASME J. Dyn. Syst., Measurement, Contr.*, vol. 115, pp. 301–308, 1993.

[8] C. H. An, C. G. Atkeson, and J. M. Hollerbach, *Model-Based Control of a Robot Manipulator*. Cambridge, MA: MIT Press, 1988.

[9] H. Asada and S.-K. Lim, "Design of joint torque sensors and torque feedback control for direct-drive arms," in *ASME Winter Annu. Meet.: Robot. Manufacturing Automat.*, vol. PED-15, Miami Beach, FL, Nov 1985, pp. 277–284.

[10] J. S. Bendat and A. G. Piersol, *Engineering Application of Correlation and Spectral Analysis*. New York: Wiley, 1980.

[11] C. W. deSilva, T. E. Price, and T. Kanade, "Torque sensor for direct-drive manipulator," *ASME J. Eng. Ind.*, vol. 109, pp. 122–127, 1987.

[12] C. Foias, B. Francis, J. W. Helto, H. Kwakernaak, and J. B. Pearson, *H infinity control theory*. New York: Springer-Verlag, 1990.

[13] B. Francis, *Lecture Notes in Control and Information science*. New York: Springer-Verlag, 1987.

[14] J. S. Freudenberg and D. P. Looze, "Right half plane poles and zeros, and design tradeoffs in feedback systems," *IEEE Trans. Automat. Contr.*, vol. 30, 1985.

[15] M. Hashimoto, "Robot motion control based on joint torque sensing," in *Proc. IEEE Int. Conf. Robot. Automat.*, 1989, pp. 256–1261.

[16] J. M. Hollerbach, I. Hunter, J. Lang, S. Umans, and R. Sepe, "The McGill/MIT Direct Drive Motor Project," in *Proc. IEEE Int. Conf. Robot. Automat.*, May 1993, pp. 611–617.

[17] K. Kosuge, H. Takeuchi, and K. Furuta, "Motion control of a robot arm using joint torque sensors," *IEEE Trans. Robot. Automat.*, vol. 6, pp. 258–263, 1990.

[18] J. Y. S. Luh, W. D. Fisher, and R. P. C. Paul, "Joint torque control by a direct feedback for industrial robot," *IEEE Trans. Automat. Contr.*, vol. 28, pp. 153–161, 1983.

[19] A. Serrarens, M. van de Molengraft, J. Mok, and L. van den Steen, "H infinity control of suppressing stick-slip in oil well drillstrings," *IEEE Contr. Syst. Mag.*, vol. 18, no. 2, pp. 19–30, 1998.

[20] J. E. Slotine and W. Li, *Applied Nonlinear Control*. Engelwood Cliffs, NJ: Prentice-Hall, 1991.

[21] D. Stokić and M. Vukobratović, "Historical perspectives and state of the art in joint force sensory feedback control of manipulation robots," *Robotica*, vol. 11, pp. 149–157, 1993.

[22] G. van der Linden and P. Lambrechis, "H infinity control of experimental inverter pendulum with dry friction," *IEEE Contr. Syst. Mag.*, vol. 13, no. 4, pp. 44–50, 1993.

[23] *System Identification Toolbox User's Guide*, The MathWorks, Natick, MA, 1995.

[24] G. Zhang and J. Furusho, "Control of robot arms using joint torque sensors," *IEEE Contr. Syst. Mag.*, vol. 18, no. 1, pp. 48–54, 1998.

Farhad Aghili received the B.Sc. and M.Sc. degrees in mechanical engineering and biomedical engineering from Sharif University of Technology, Tehran, Iran, 1988 and 1991, respectively. He received the Ph.D. degree in mechanical engineering from McGill University, Montreal, QC, Canada, in February 1998.

Currently, he is a Research Scientist at Canadian Space Agency, where he has worked on the International Space Station program since January 1998. From 1994 to 1997, he was a Research Engineer at MPB Technologies, Montreal. His main areas of interest include robotics and automatic control.

Martin Buehler (S'85–M'90) received the Ph.D. degree in electrical engineering from Yale University, New Haven, CT, in 1990.

He studied legged locomotion as a Postdoctoral Associate at the Artificial Intelligence Laboratory, Massachusetts Institute of Technology, Cambridge. In 1991, he joined McGill University, Montreal, QC, Canada, as a Junior Industrial Research Chair, and is currently an Associate Professor there. His main research interests include motor control, legged locomotion, biomimetics, energetics, actuators, and robot design and control. He is an Associate Editor for the IEEE TRANSACTIONS ON ROBOTICS AND AUTOMATION.

John M. Hollerbach (M'85–SM'92–F'96) received the B.S. degree in chemistry in 1968 and the M.S. degree in mathematics in 1969 from the University of Michigan, Ann Arbor, and the S.M. and Ph.D. degrees in computer science from the Massachusetts Instutute of Technology, Cambridge, in 1975 and 1978, respectively.

From 1978 to 1982, he was a Research Scientist and from 1982 to 1989, he was on the faculty of the Department of Brain and Cognitive Sciences and a member of the Artificial Intelligence Laboratory at MIT. From 1989 to 1994, he was the Natural Sciences and Engineering/Canadian Institute for Advanced Research Professor of Robotics at McGill University, jointly in the Departments of Mechanical Engineering and Biomedical Engineering. He is currently Professor of Computer Science, and Adjunct Professor of Mechanical Engineering, at the University of Utah. He was a Technical Editor of the IEEE TRANSACTIONS ON ROBOTICS AND AUTOMATION from 1989–1994. His research interests include robotics, virtual reality, and microelectromechanical systems.

Dr. Hollerbach received an NSF Presidential Young Investigator Award in 1984. In 1988, he was named a Fellow of the Canadian Institute for Advanced Research. He was the Program Chairman of the 1989 IEEE International Conference on Robotics and Automation, a member of the Administrative Committee of the IEEE Robotics and Automation Society from 1989 to 1993, and Treasurer of the IEEE/ASME JOURNAL OF MICROELECTROMECHANICAL SYSTEMS from 1992 to 1997. He was a member of the 1994 to 1995 National Research Council Committee on Virtual Reality Research and Development. Presently he is Editor of the *International Journal of Robotics Research*, a Senior Editor of *Presence: Teleoperators and Virtual Environments*, and a Governing Board member of the electronic journal *Haptics-e*.